Proceedings of ASME Turbo Expo 2011
GT2011
June 6-10, 2011, Vancouver, British Columbia, Canada

GT2011-46853

FLEXIBLE NON-INTRUSIVE HEAT FLUX INSTRUMENTATION ON THE AFRL RESEARCH TURBINE

Richard J. Anthony, John P. Clark, Stephen W. Kennedy, John M. Finnegan
Air Force Research Laboratory, Turbine Branch, Propulsion Directorate
WPAFB, OH, USA

Dean Johnson, James Hendershot, James Downs
Florida Turbine Technologies, Jupiter, FL

ABSTRACT

This paper describes a large scale heat flux instrumentation effort for the AFRL HIT Research Turbine. The work provides a unique amount of high frequency instrumentation to acquire fast response unsteady heat flux in a fully rotational, cooled turbine rig along with unsteady pressure data to investigate thermal loading and unsteady aerodynamic airfoil interactions. Over 1200 dynamic sensors are installed on the 1 & ½ stage turbine rig. Airfoils include 658 double-sided thin film gauges for heat flux, 289 fast-response Kulite pressure sensors for unsteady aerodynamic measurements, and over 40 thermocouples. An overview of the instrumentation is given with in-depth focus on the non-commercial thin film heat transfer sensors designed and produced in the Heat Flux Instrumentation Laboratory at WPAFB. The paper further describes the necessary upgrade of data acquisition systems and signal conditioning electronics to handle the increased channel requirements of the HIT Research Turbine. More modern, reliable, and efficient data processing and analysis code provides better handling of large data sets and allows easy integration with the turbine design and analysis system under development at AFRL. Example data from cooled transient blowdown tests in the TRF are included along with measurement uncertainty.

INTRODUCTION

The Air Force Research Laboratory (AFRL) has been heavily involved in design-code validation for a number of years. Many of the efforts undertaken to date, however, were restricted by proprietary considerations [e.g. 1, 2]. In late 2002, the Scientific Advisory Board of the US Air Force recommended that the laboratory commit itself to turbine research that benefits the industry as a whole instead of a single company. Accordingly, it was recognized that non-proprietary geometries were a pre-requisite to such work. Therefore, an

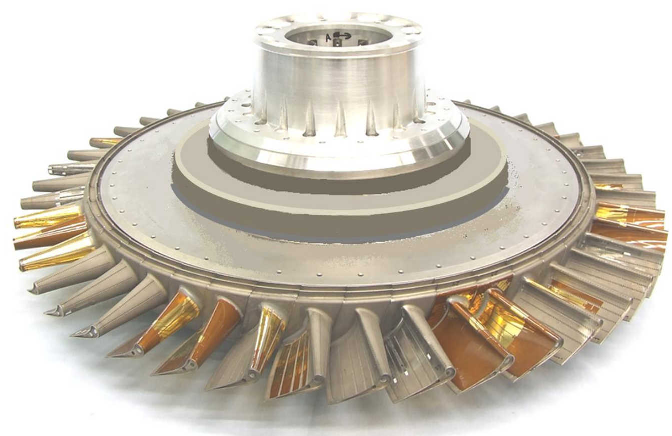

Figure 1: Completed HIT Research Turbine Rotor with Custom Thin Film Instrumentation.

effort was undertaken to create an aerodynamic design system for turbine airfoils at the laboratory to enable the definition of government-owned geometries [3]. This effort, teamed with custom in-house instrumentation capabilities, led to the completion of the full scale, non-proprietary high pressure turbine test hardware shown in Figure 1.

The turbine analysis system developed with this effort is consistent with gas turbine industry standards, and it is illustrated as a design loop in Figure 2. The system was used to design the High Impact Technologies Research Turbine (HIT RT). The HIT RT is a stage-and-one-half high pressure turbine that is consistent with a dual-spool engine that has an Overall Pressure Ratio (OPR) of 40 and is governed by basic cycle parameters that are shown emboldened in Table 1 for the constraint of a fixed flowpath. While meanline design studies

NOMENCLATURE

A flowpath area [m^2]
a thickness [m]
c specific heat [kJ/kg K]
h convective heat transfer coefficient [W/m^{2}K]
I_s constant current supplied by source [Amps]
k thermal conductivity [W/mK]
N rotor speed [rpm]
q heat flux [W/m^2]
R resistance [Ω]
R_0 resistance at T_0 [Ω]
Re_x local Reynolds Number
s Laplace Transform variable
T temperature [K]
T_0 reference temperature [K]
t time [s]
U mean freestream velocity [m/s]
V voltage change during test [volts]
V_0 voltage across film at T_0 [volts]
x streamwise coordinate from leading edge [m]
z spanwise coordinate from sidewall [m]
α thermal diffusivity (= $k/\rho c$) [m^2/s]
α_R temperature coefficient of resistance [1/°K]
ρ density [kg/m^3]
ω angular frequency [radians/s]

involved both complete spools of the engine, detailed aerodynamic design was undertaken only for the inlet guide vane (1V), the high pressure turbine blade row (1B), and the guide vane of the low pressure turbine (2V). Complete details of the aerodynamic design are available in [3] and [4]. Preliminary CFD results are discussed in Johnson et. al. [5].

The scope of this particular paper focuses on instrumentation developments required to enable collection of unsteady heat-flux data for the validation of state-of-the-art durability design systems. The paper provides a description of initial code validation requirements, instrumentation overview, thin-film sensor background, calibration, completed turbine airfoils, and example data collected in the Turbine Research Facility (TRF) at Wright-Patterson Air Force Base. This paper is intended to serve as a reference for ongoing and future studies using the HIT Research Turbine hardware.

The experimental testing performed here is comparable and shares some lineage with past studies at the MIT Blowdown Turbine Facility [6,7,8], and the Ohio State University Gas Turbine Laboratory Turbine Test Facility (formerly at Calspan) [9,10,11]. The reader is also referred to rotating tests with heat transfer instrumentation at the Von Karman Institute's Compression Tube Turbine Test Facility (CT3) in Belgium [12,13,14]. Measurement techniques described in this paper share lineage with past work at the University of Oxford Osney Laboratory [15] and the Oxford Turbine Research Facility (formerly at QinetiQ) [16]. Additional references on measurement techniques are given in following sections of the paper.

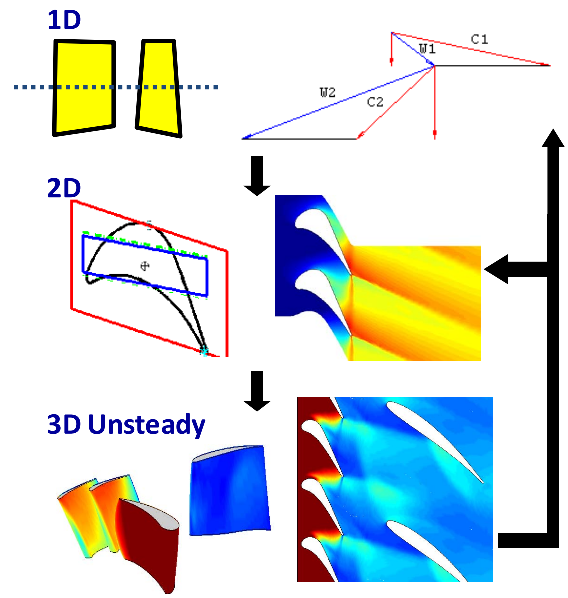

Figure 2: A Typical Iterative Design Loop for Turbine Airfoils.

Table 1: Cycle data (**emboldened**) and meanline design parameters (plain text) for the HIT RT.

T3 (K)	**222**			
T4 (K)	**444**			
Inlet Flow Parameter [(kg/s) K$^{1/2}$ / kPa]	**1.13**			
	1V	1B	2V	2B
Work Coefficient [(g J ?h) / U_{mean}^2]	----	2.08	----	2.01
Flow Coefficient ($C_{x,exit}$ / U_{mean})	----	0.71	----	1.2
Efficiency (%)	----	87.3	----	91.7
Pressure Ratio (Total-Total)	**----**	**3.75**	**----**	**1.85**
Reaction (%)	----	49.5	----	55.0
N / $T_{t,in}^{1/2}$ (RPM / K$^{1/2}$)	----	361	----	279
AN^2 x10^{-6} (m RPM)^2 [Engine / Rig]	----	37 / 8.4	----	21 / 4.8
Exit Mach Number	0.88	1.30 (rel)	0.89	0.94 (rel)
Turning (degrees)	77	115	11	80
Percent Cooling	**7**	**4**	**5**	**2**
Airfoil Count	23	46	23	69
Zweifel Coefficient	0.85	1.13	0.4	1.25

INSTRUMENTATION OVERVIEW

First an overview of the instrumentation package is given, followed by a closer look at the custom non-commercial heat flux sensors installed on the high pressure turbine (HPT). Overall, more than 1200 dynamic sensors are installed on the Research Turbine test rig. The airfoils alone include 658 thin film sensors for double-sided heat flux measurements, 289 fast-response Kulite pressure sensors, and over 40 thermocouples. Commercial sensors include Omega Type-E thermocouples using GE Kaye external ice point references. Airfoil unsteady pressure measurements are predominantly Kulite LQ-062 high bandwidth transducers mounted flush with the airfoil surface. These are modified to capture bandwidth up to approximately 75kHz in order to provide detailed mappings of unsteady airfoil pressures.

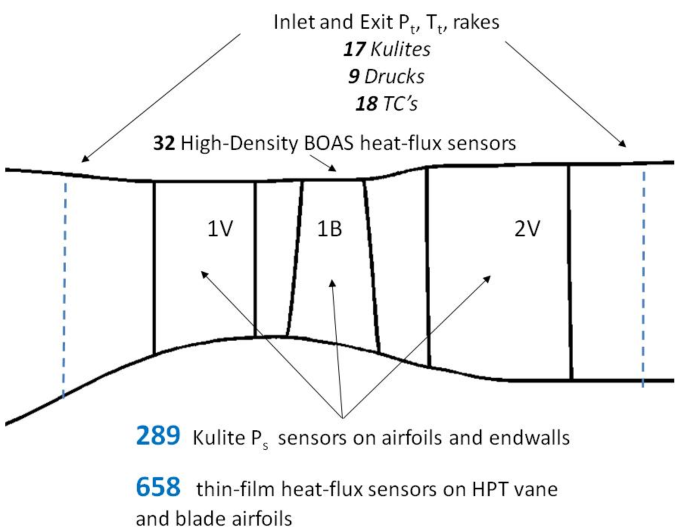

Figure 3: Instrumentation Requirements for the HIT Research Turbine

In addition to the airfoils, there are approximately 200 sensors used for traversing rakes, two independent cryogenic cooling systems, and dynamic response monitoring of the rig. Four inlet and four exit traversing rakes provide fast response pressure and temperature profiles upstream and downstream of the airfoils. Several proximity probes and accelerometers are included on the new drive system to monitor rotordynamics and vibration.

The effort described here is unique due to the amount of high bandwidth sensors being nearly an order of magnitude greater than past turbines tested in the TRF. The leap in sensor count also led to a substantial modernization and expansion of the TRF data acquisition systems. Additional TRF modernization efforts, which are outside the scope of this paper, include a significant rotordynamic re-design of the TRF drive system with support from Florida Turbine Technologies (FTT), Inc. This and several other projects are part of a recent major upgrade of the Turbine Research Facility at WPAFB.

CUSTOM HEAT FLUX INSTRUMENTATION

Unsteady code validation required 329 double-sided heat flux measurement locations on multiple HPT vane and rotor airfoils. Since each double-sided gauge requires both a top and bottom sensor, 658 individual high bandwidth thin film sensors were required.

To meet the quantity with a limited budget, sensors were designed and fabricated in the Heat Flux Instrumentation Laboratory at AFRL. The laboratory is a class 10,000 clean room that allows custom sensor design flexibility and fast turnaround at relatively low cost. It produces various devices for high bandwidth heat transfer measurements and non-intrusive flow control studies [17]. The following describes basic operation and calibration of the thin film heat flux gauges, followed by examples of the completed vane and blade airfoils. Example data from full scale blowdown testing are given at the end of the paper.

Thin Film Sensor Background

Thin film heat flux instrumentation has been in use for several decades. Early applications were in short duration testing for hypersonic re-entry vehicles in the 1950's [see 18, 19, 20]. With the rise of relatively low cost transient turbine test facilities, the technique found application in turbomachinery research (see Schultz and Jones [21,22] at Oxford, Epstein et. al. [23] at MIT, Dunn [24] and Haldeman et. al. [25] at Ohio State University, formerly Calspan), and Iliopoulou and Arts [26], Von Karman Institute. The sensors for the current program are produced with a new procedure that improves gauge durability and does not produce regulated chemical waste. Each double-sided heat flux gauge is made up of two thin film sensors which are individually calibrated. A simple schematic of a conventional thin film sensor is shown in Figure 4.

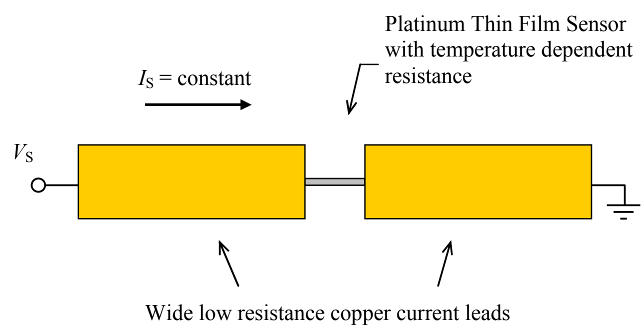

Figure 4: Schematic of a conventional thin film heat flux sensor

The platinum thin film acts as a resistance thermometer. Changes in film temperature result in changes in sensor resistance. A constant current is passed through the thin film and changes in resistance are monitored by changes in the output voltage V_S. The resistance of the wide copper leads is very small relative to the platinum sensing film, so that only the sensor resistance significantly effects the change in supply voltage V_S. The voltage change across the sensing film due to a change in temperature $T - T_0$ is then given by

$$\Delta V = V_0\, \alpha_R (T - T_0) \tag{1}$$

where α_R is the thermal coefficient of resistivity of the film determined by calibration. Frequency response of the thin films can be up to 200kHz with appropriate signal conditioning electronics. This is adequate to measure unsteady turbulent fluctuations in the rig that are typically less than 100 kHz.

Sensor Calibration

Thermal calibration data was collected for all 658 sensors on the HIT Research Turbine. To accomplish this, an automated high channel count, high temperature range, thermal calibration system was developed. The apparatus includes a Fluke Hart-Scientific constant temperature controlled bath with programmable ramp and soak profiles and sub-zero temperature capability. Custom Matlab code linked with Labview controls data collection and analysis. The system uses a 6 ½ digit digital multimeter with a programmable 96 channel multiplexer in a PXI chassis with embedded controller from National Instruments. A laboratory standard calibrated RTD probe is used to measure the bath temperature. The new system allows multiple airfoils to be calibrated at the same time automatically.

Multiple ramp and soak steps are run with the bath following a temperature vs. time staircase profile. Film resistance measurements are recorded on all airfoils after they reach thermal equilibrium at each temperature set point. Multiple resistance measurements are recorded and averaged at the end of each step (i.e. when bath fluid remains steady within +/- 0.01 °F and film resistances no longer vary with time). Soak time for each step depends on the hardware in place, and in some cases, may last several hours at each step to ensure film resistances are recorded at thermal equilibrium.

An example sensor calibration plot is shown in Figure 5. Measurement points as low as -40°C (-40°F) for some sensors and up to 104°C (220°F) for others were collected. Note different time intervals of a TRF cooled blowdown run may drive temperature both cooler or warmer than the turbine's initial ambient condition. This is dependent on gauge location and the cooling flow test sequence. The new sub-zero capability allows full range calibration of fully cooled hardware for TRF.

To determine the thermal coefficient of resistivity, α_R, used in equation 1 for each film, the temperature-resistance plot is normalized by $(R\text{-}R_{20})/R_{20}$ and plotted versus temperature change in degrees C (Figure 8). R_{20} is the reference resistance of the film at room temperature (T_{20} = 20°C). The platinum films are relatively linear over a large range; resulting in R^2 values greater than 0.999 well over 100 °C span. Error bars for Figure 7 are based on 95% uncertainties of approximately 0.008 ohms and 0.01 F which are about the size of the data markers. Individual calibration plots are created for each sensors. In the end, about 6000 temperature-resistance pairs were collected, analyzed, and documented, for the HIT RT.

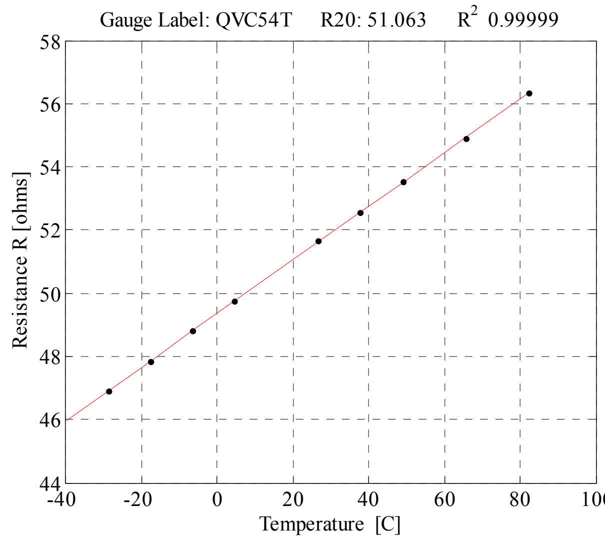

Figure 5: Thermal Calibration Points for a Single Thin Film Sensor

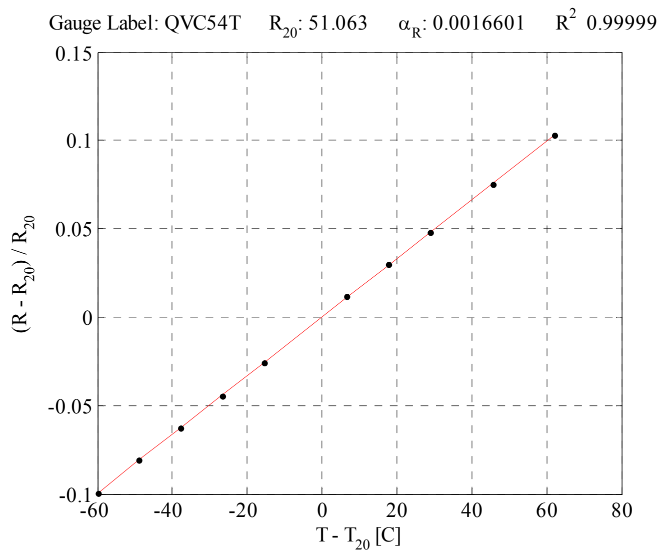

Figure 6: Thermal Coefficient of Resistance α_R determined for each individual sensor

Thermal properties of the polyimide substrate between the top and bottom thin film sensors are also measured and used for time accurate solution of the unsteady heat equation to determine surface heat flux. A summary of the thermal property measurements with quantified uncertainty values are given in Table 2. Substrate thermal conductivity is measured with a guarded-comparative-longitudinal heat flow technique based on ASTM standard E-1225. Specific heat measurements are made in accordance with ASTM Standard E 1269 and density measurements are made in accordance with ASTM Standard C 303-02. Actual substrate thermal properties may vary from the manufacturer's stated bulk values. Thermal conductivity, for example, was found to be slightly higher than quoted. Thermal properties verified in these procedures are next used to convert transient thin film temperature signals into unsteady heat flux data.

Table 2: Double-Sided Gauge Measurement Uncertainty Values in Figures 8 & 9 at 8 sec

Parameter	Symbol	Value	Standard Uncertainty u	Expanded Uncertainty *95% Confidence interval* ($2u$)
Thickness	a	51.1 μm	0.9 μm	1.8 μm
Specific Heat	c	1136 kJ/kg K	5.7 kJ/kg K	11.4 kJ/kg K
Thermal Conductivity	k	0.179 W/mK	0.0064 W/mK	0.0128 W/mK
Density	ρ	1410 kg/m^3	24.7 kg/m^3	49.4 kg/m^3
Temperature Coefficient of Resistance	α_R	1.662 x10^{-3} K^{-1}	2.06 x10^{-6} K^{-1}	4.12 x10^{-6} K^{-1}
Surface Temperature change	T	52.94 K	0.82 K	1.64 K
Heat Flux	q	5.36 x10^4 W/m^2	4.4 x10^3 W/m^2	8.8 x10^3 W/m^2

Surface Heat Flux Conversion

During experiments, the measured thin film temperature signals are converted to heat flux either numerically or, in the past, by an electrical analogue circuit [27]. Surface heat flux in this experiment is derived from the double-sided thin film construction shown in Figure 7. For slowly varying or steady flow facilities, the heat flux rate may be calculated simply using

$$q = k/a\,(T_1 - T_2) \tag{2}$$

where T_1 and T_2 are the top and bottom thin film temperatures and a is the dielectric thickness. In short duration transient test rigs like TRF, however, the full unsteady linear differential equations governing heat conduction through the flexible dielectric layer must be analyzed (see Doorly and Oldfield [28]). This is necessary to fully resolve the true high frequency surface heat flux events occurring in unsteady turbine flows.

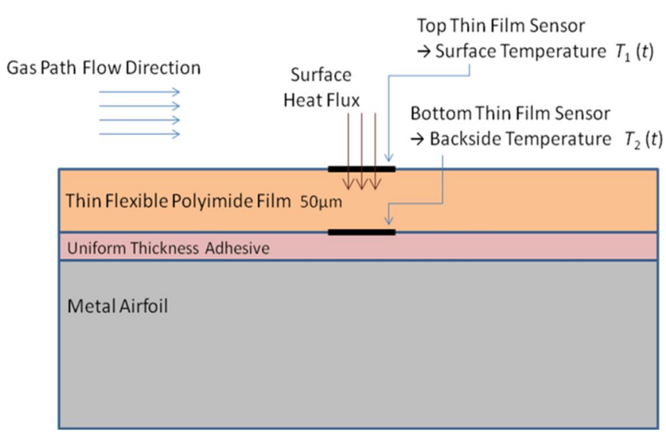

Figure 7: Double-Sided Thin Film Heat Flux Sensor Diagram

Analysis of unsteady heat conduction for a double sided sensor may be approximated by several methods. The technique employed in this program follows a more recent and computationally efficient digital impulse response filtering routine which approximates the solution of the differential equations governing one dimensional heat conduction through a double sided gauge The digital filtering technique was implemented with Matlab-based signal processing routines in Anthony et al. in 1999 [29]. A detailed reference on the digital impulse response methods are given in the journal article by Oldfield [30]. Example data showing temperatures from both top T_1 and bottom T_2 sensors and the resulting heat flux trace for a blowdown run in the TRF are given later in the paper.

Instrumented Vane Airfoils

CFD design predictions defined locations for unsteady heat flux measurements on the HPT vanes. Multiple vane passages were instrumented after careful layout, manufacture, and installation of fast-response, double-sided gauges. Examples are shown in Figures 8 through 12. Data from the gauge location identified in Figure 8 are plotted in Figures 22 and 23.

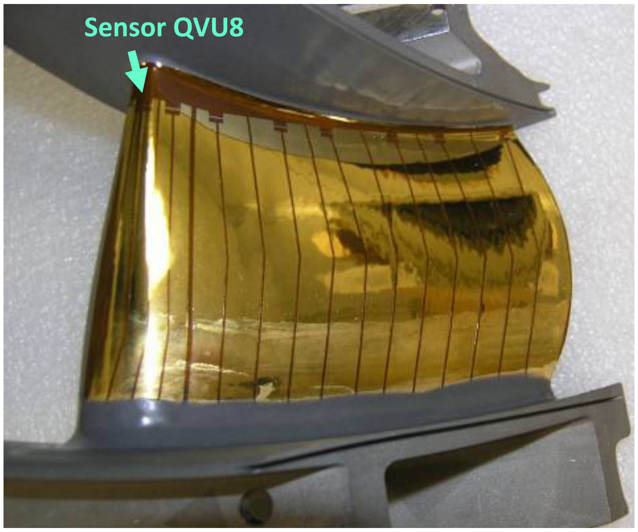

Figure 8: Double-Sided Vane Sensors Near the ID Endwall

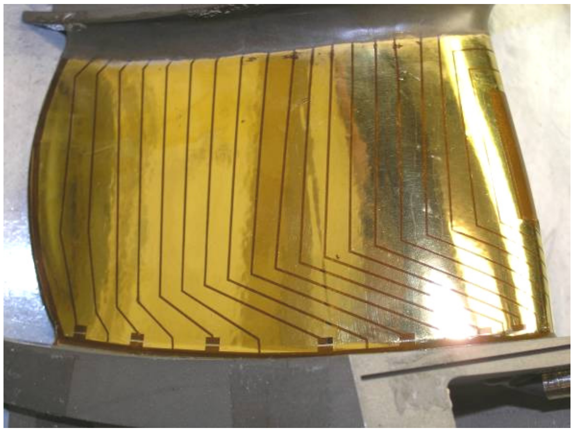

Figure 10: Double-Sided Vane Sensors Near OD Endwall

One hundred eighty gauge locations (360 thin film sensors) are laid out across multiple airfoil span and chord locations. Flexible films wrap around leading edges and extend to trailing edges at differing spans; from the ID endwall (Figure 8) to the OD endwall (Figure 10). Copper film leads exit out the opposite endwalls in these two cases to prevent any disturbance near the endwall corner sensing locations. Airfoil span locations of 5%, 25%, 50%, 72%, 90%, and 95% are instrumented on both the suction side and pressure side of each vane passage. Figure 11 shows 9 gauge locations along a 50% span suction side.

A unique advantage of the flexible films is they are installed with minimal intrusion to both the metal airfoil and the aerodynamic surface under study. The polyimide film substrate adheres like a smooth layer of skin that does not negatively disturb the boundary layer. Figure 11 shows the thin, non-intrusive film on a cooled pressure side vane with sensors at 95% span near the ID endwall.

Figure 11: Double-Sided Vane Sensors Along 50% Span

Figure 12 shows the completed and installed vane set at the end of the vane test program following many long duration, large Reynolds number blowdown tests carried out over the course of a year. The photo shows the positive result of process changes and enhancements to significantly improve robustness of the films. In all, a total of 12 passages were fully instrumented with double-sided thin film heat flux gauges. Additional vane airfoil instrumentation includes 34 fast

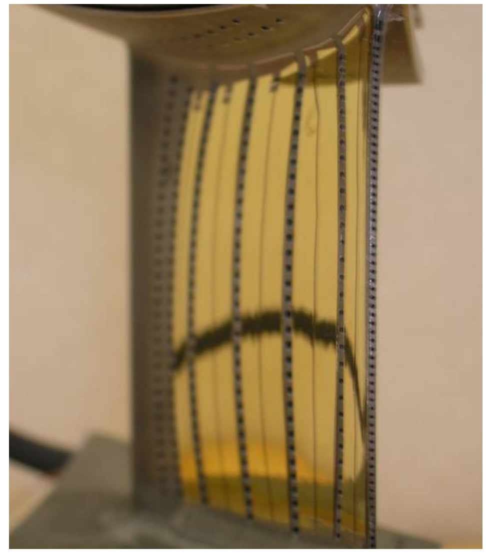

Figure 9: Trailing Edge Looking Upstream of a Cooled Vane with Sensors Near the ID Endwall

response Kulite pressure probes for unsteady aero measurements and 32 Type E thermocouples. The completed vanes were carefully assembled and wired at FTT and shipped to AFRL to begin testing in 2010. A brief description of the vane test blowdown procedure with preliminary data is given later in the paper.

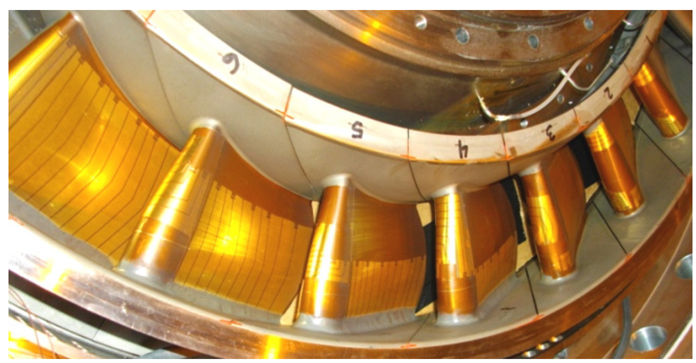

Figure 12: Completed and Installed Vane Ring Photo taken after a yearlong series of blowdown testing

Instrumented Rotor Airfoils

While the HIT RT first stage vane was completed, installed, and tested, concurrent work continued on the HIT RT HPT rotor. In addition to the vane sensors, 99 double-sided heat flux gauge locations (198 thin film sensors) were designed, manufactured, installed, and calibrated for the Research Turbine rotor blades. An example of a completed cooled pressure side blade is shown in Figure 13. Manufacturing capability was pushed in some cases to place sensors in very tight locations. Sensors as small as 1mm x 0.1mm wide were carefully fabricated and successfully installed between leading edge cooling holes on some HPT rotor blades.

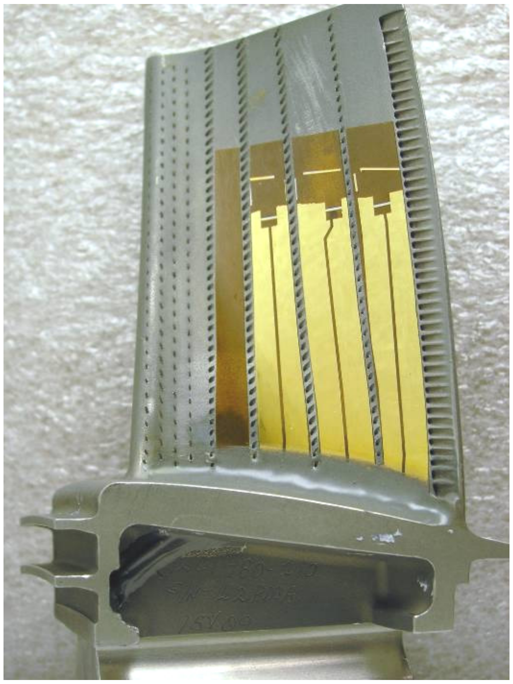

Figure 13: Cooled Pressure Side Rotor Blade with Double-Sided Films

Figure 14 shows an example of unique measurement locations near the tip of a cooled HPT rotor blade. Locating the sensors near the tip and between cooling holes required no interference with blade cooling geometry; nor did it require any machining or intrusion of the thin-walled airfoil geometry near the trailing edge tip corner.

The final HPT rotor instrumentation includes blade passages with both pressure side and suction side sensing films along with non-intrusive blade platform films as well (Figure 15). Rotating platform and tip flows are targeted areas where design CFD models can struggle to make accurate heat transfer predictions. Measuring unsteady rotating 3-D boundary layer effects in these areas can be critical since unrealistic predictions

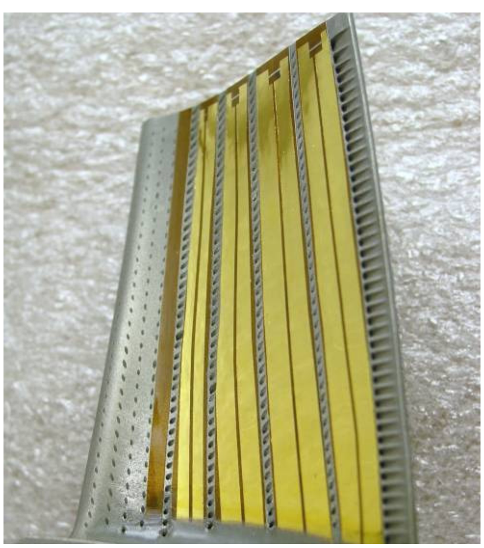

Figure 14: Sensors Near the Tip of a Fully Cooled Rotor Blade

in such areas can lead to significant shortfalls in component life. This, in turn, can greatly increase turbine engine maintenance and overhaul costs, or in some cases, increase risk of unanticipated engine failure.

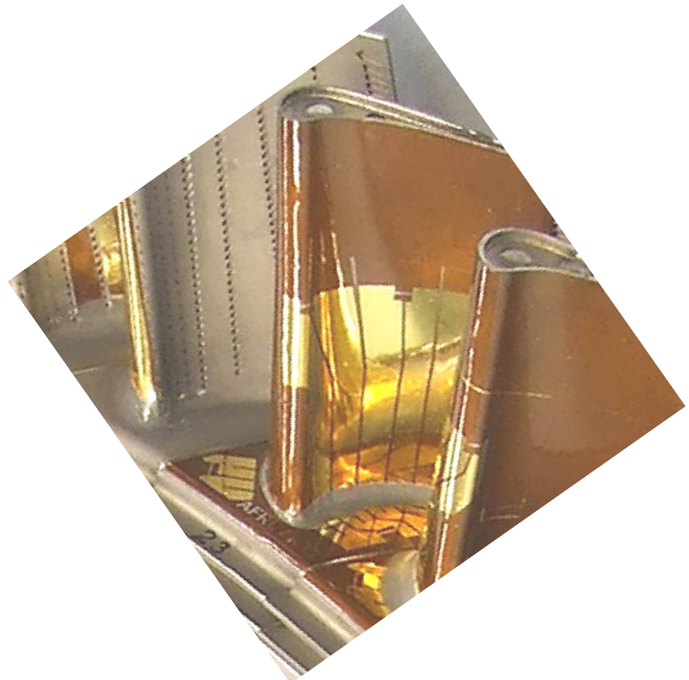

Figure 15: Double-Sided Blade Platform Films with Instrumented Pressure and Suction Sides in the Rotating Turbine Blade Passages

Similar to the vane, the HIT RT rotor was carefully assembled and wired at FTT and mated to a new shaft drive assembly. The completed rotor is shown in Figure 1. In addition to the thin films described here, the completed HPT rotor also includes 75 fast response Kulite LQ-062 pressure probes for unsteady aero measurements and multiple high-density disk broach slot heat flux arrays.

High Density Thin Film Arrays

A different type of heat flux sensing array was designed and used in selected disk broach slots, and the rotor Blade Outer Air Seal (BOAS). These areas are instrumented with high-density thin film heat flux arrays developed by Anthony et.al [29] and described below.

Figure 16 shows a schematic of a high density heat flux imaging array similar to that used on the HIT RT BOAS. The platinum thermal resistance acts similarly to the conventional films described in Figure 4; however, film sense and excitation leads are separated. Since the voltage sense leads do not carry current, they may be made thinner, and several films may be joined closely together to form an array. The high density arrays can provide both high spatial resolution as well as high bandwidth, making them uniquely capable of capturing detailed unsteady heat transfer events occurring over a surface. Figure 17 shows an example of a 2-D (span-time) image of surface heat flux events crossing over an imaging array on the leading edge of a wind tunnel model subjected to freestream turbulence [31]. In this example, unsteady boundary layer streaks and spots are seen at relatively low Reynolds number. A similar imaging array on the HIT RT BOAS is installed to capture unsteady heat flux events as the rotating blade tips pass by. More detail and additional experiments using this high bandwidth heat flux imaging technique are given in [32, 33].

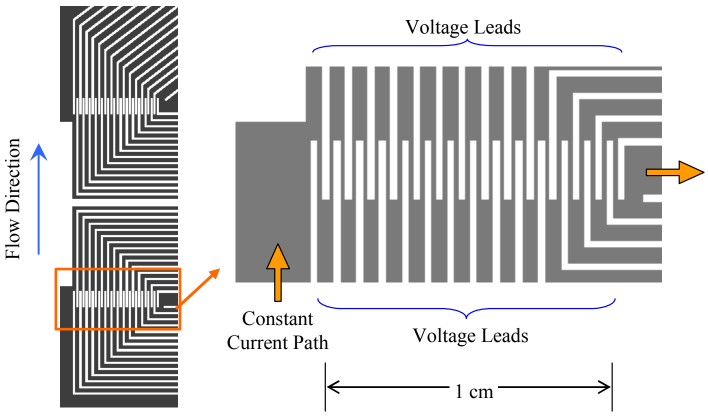

Figure 16: Schematic of a High Density Heat Flux Imaging Array

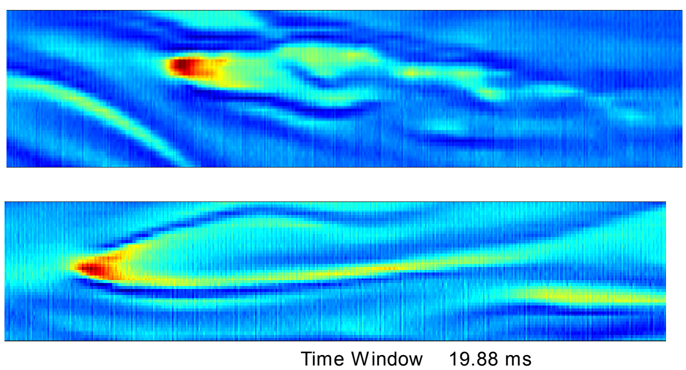

Figure 17: Example Time-Resolved Heat Flux Data from a High Density Heat Flux Imaging Array on a Leading Edge Subjected to Freestream Turbulence (Anthony et. al. [31])

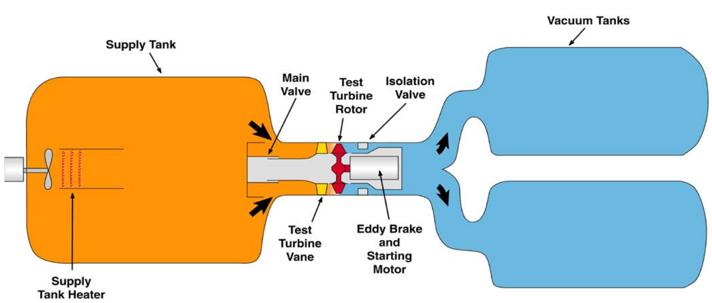

Figure 18: Diagram of the Turbine Research Facility at WPAFB

TURBINE RIG TESTING

The paper so far has given a descriptive overview of the custom instrumentation designed, produced, and installed for the first HIT Research Turbine test program. The remainder of the paper briefly describes the transient, short duration test facility and the analog/digital signal processing and data acquisition upgrades performed to run the full 1 & ½ stage HIT Research Turbine. Example test data from the new films and data acquisition systems are shown.

Test Facility

All measurements with the full 3D geometry of the HIT RT take place in the Turbine Research Facility (TRF) at AFRL [1]. The TRF is a transient blowdown wind-tunnel that allows for measurements of unsteady heat transfer and aerodynamics on full scale engine hardware. It matches relevant aerodynamic and heat transfer parameters including Reynolds number, Prandtl number, corrected speed, pressure and temperature ratios to test scaled engine conditions. The rig includes upstream and downstream traverse rings and independent cryogenic cooling circuits for cooled turbine studies. A simple schematic of the facility is shown in Figure 18.

Research Turbine Vane testing was carried out in TRF in 2010. Multiple series of blowdown tests were run to characterize the vane and assess performance of the cryogenic cooling systems. Full 1 & ½ stage testing with the rotor is planned to begin in 2011. The TRF test section with the HIT RT vane installed is shown in Figure 19. The large heated supply tank is on the left. When the main valve opens, flow is expanded left to right through the turbine test section and into the large evacuated dump tanks. Cryogenic cooling lines are seen feeding into various OD clock locations, while a separate, and larger, cryogenic cooling circuit is plumbed inside the rig to feed the ID cooling flowpaths. Main flow blowdown durations for the vane-only program are between 3 to 5 seconds. Blowdown durations with the rotor are limited to under 2.5 seconds depending on torque.

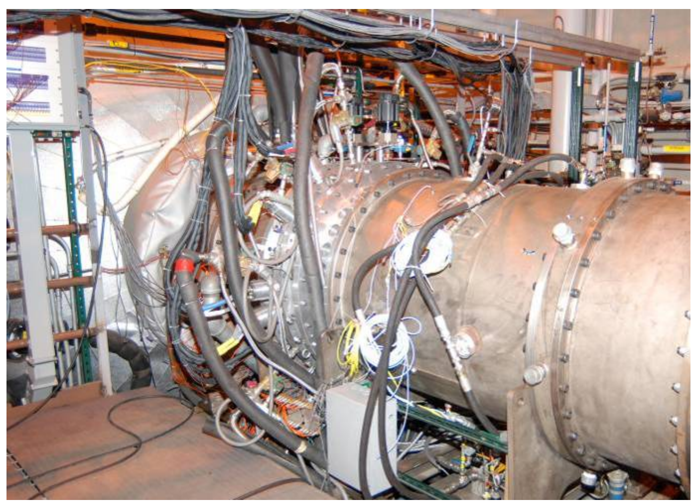

Figure 19: Test Section of the AFRL Turbine Research Facility with the Cooled Research Turbine Vane Installed for Testing

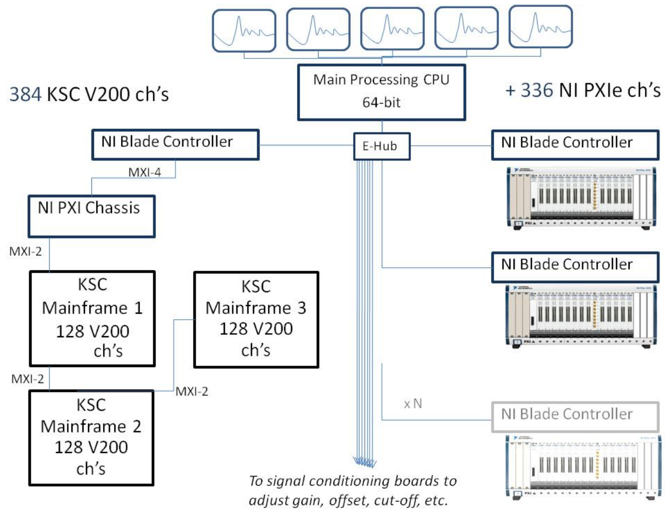

Figure 20: Updated Data Acquisition Expansion Scalable to Higher Channel Count

Data Acquisition and Signal Processing Upgrades

The variety and quantity of sensors on the HIT RT required a more modern, reliable data processing and analysis system. The requirements for the HIT RT created a unique challenge for TRF where the total number of sensors outnumbered the total available data channels by more than 3:1. A complete renovation and expansion of the high speed data acquisition system in TRF has been undertaken.

First, a collaborative effort between AFRL and the Mathworks, Inc helped develop a versatile Matlab driver interface for the existing 384 KSC VXI V200 A/D channels. This enabled users to quickly set-up, acquire, process, display, and efficiently analyze very large data sets from the TRF. Furthermore, this allowed easy integration with the digital signal processing and analysis techniques used already in Anthony et al [31, 33] and the turbine design and analysis system developed by Clark et al. [3]; both programmed predominantly in Matlab.

Second, to meet the large additional channel expansion requirement, new NI PXI-Express A/D cards are added along with versatile signal conditioning hardware from Precision Filter, Inc. Model 280114 signal conditioning cards feature programmable current or voltage excitation for either Kulites or thin film RTD's, along with programmable gains, offset, filtering, and sensor fault detection. Additional multi-function, digitally controlled, signal conditioning boards were also developed in-house to provide lower-cost channel expansion options.

Figure 20 shows a schematic of the expanded data system which integrates the existing 384 VXI channels on the left with the several hundred added NI PXI-Express channels on the right. The data acquisition and signal processing upgrade is part of a much larger, ongoing modernization effort in the TRF carried out in the past two years.

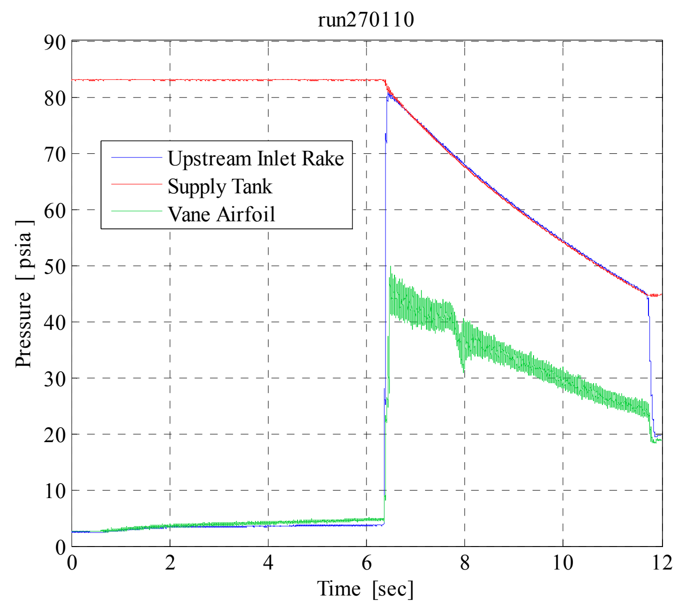

Figure 21: Pressures During TRF Blowdown with an Initial Precool Period

Example Vane Test Data

Figures 21 thru 23 show preliminary data collected from a TRF blowdown test with the HIT RT Vane installed. In this particular test case, cooling flow is started early to significantly precool the lines leading to the rig, then shortly after 6 seconds the fast acting main valve opens and the heated main flow rushes though the test section till the main valve is again closed just before 12 seconds. As the supply tank discharges there is a gradual decrease in Reynolds number over the test period. Note the dip in vane airfoil pressure near 8 seconds is due to the passing of an upstream traverse rake.

Figure 22 shows top and bottom temperature traces from a double-sided thin film gauge located on the leading edge of an uncooled vane near the ID endwall. The airfoil with this sensor identified is shown in Figure 8. The top surface film temperature rises higher and faster when the main valve opens, with the bottom-side temperature lagging as the main flow heat flux penetrates the airfoil surface. These two traces are used to calculate the surface heat flux trace shown in Figure 23. The transient heat flux trace shown is the output of the impulse filter response method described earlier in the paper [30]. It can be seen in this case there is slight cooling at the surface during the initial precool period, followed by a substantial rise in heat flux as the initial main valve shock passes through the test section. Heat flux then steadily decreases during the blowdown as the Reynolds number gradually decreases. The gradual decay of surface heat flux tracks well with the drop in vane pressure shown in Figure 21 as expected.

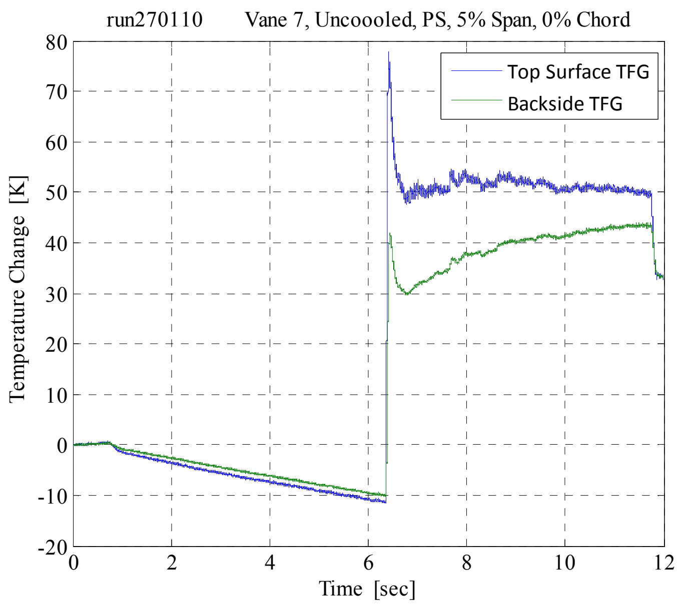

Figure 22: Double-Sided Thin Film Temperature Traces From a Vane Test Run with Pre-Cooling and Main Valve Open Just After 6 Seconds

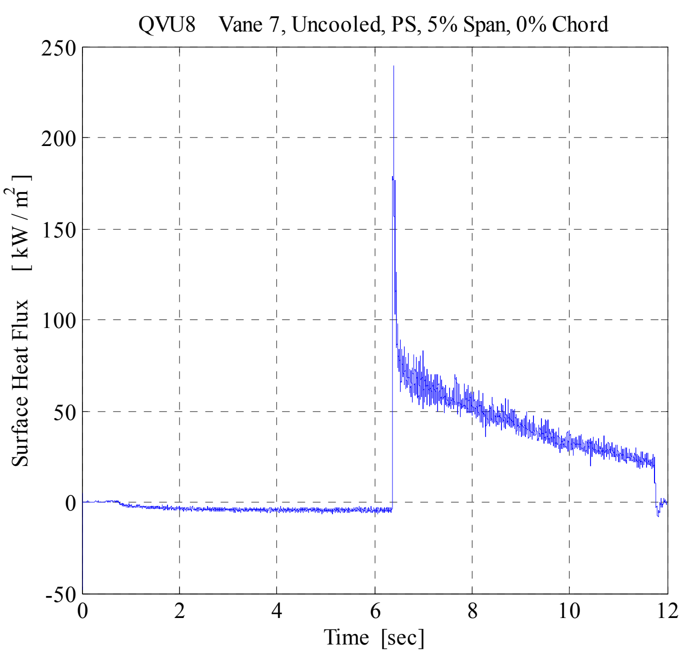

Figure 23: Surface Heat Flux Trace Calculated from Double-Sided Thin Film Signals in Figure 22

Uncertainty estimates for data plotted in Figures 22 and 23 are given in Table 2. Propagation of uncertainty is based on guidelines for tracking standard uncertainty published by NIST [34]. Uncertainty propagation is calculated separately for each individual sensor. Table 2 summarizes uncertainty values for gauge QVU8 at t=8 sec. Uncertainty may vary for different sensors under different run conditions. Factors affecting estimates for a certain gauge may include varying channel-to-channel calibration coefficients and signal-to-noise ratio.

CONCLUSION

This paper describes the large scale thin film heat flux instrumentation for the AFRL HIT Research Turbine. The HIT RT instrumentation effort provides a unique amount of high frequency unsteady measurement capability; nearly an order of magnitude greater than past turbine rigs run in the TRF. More than 1200 dynamic sensors are installed on the 1 & ½ stage turbine. Airfoils alone include 658 thin film sensors for double-sided heat flux measurements, 289 fast-response Kulite pressure sensors for unsteady aerodynamic measurements, and over 40 thermocouples. Over 200 other dynamic sensors are distributed throughout the turbine rig.

Custom patterned double-sided thin film heat flux gauges were designed, manufactured, and calibrated in the Heat Flux Instrumentation Laboratory at WPAFB. The flexible film sensors provide high bandwidth heat flux measurements with minimal intrusion to the airfoil geometry or the surrounding flowfield. Vane and rotor blade passages were carefully instrumented across multiple chord and span locations. Double-sided films are also applied to rotor blade platforms. High-density thin film arrays are applied to both HPT disk broach slots, and blade outer air seals.

An automated thermal calibration system was developed and explained to calibrate multiple airfoils simultaneously over a wide temperature range. Sub-zero temperature capability allows full range calibration of cooled hardware for TRF. Over 6000 thermal calibration measurements were collected and stored for all sensors. Uncertainty estimates for the parameters affecting heat flux determination are summarized in the paper.

The leap in sensor requirements also led to a substantial modernization and expansion of the TRF data acquisition systems. More modern, powerful, and reliable data processing and analysis code provides better handling of large data sets and allows easy integration with the turbine design and analysis system under development at AFRL.

Research Turbine Vane testing began in TRF in 2010. Several blowdown tests were run to characterize the vane and assess performance of the cryogenic cooling systems. Full 1 & ½ stage testing with the rotor is scheduled to begin in 2011.

ACKNOWLEDGMENTS

This work required a team effort across multiple organizations. The authors acknowledge the work of Robert Free of Universal Technology Corporation (UTC) and Steve Brittain of FTT for their careful wiring and assembling of the hardware, and Gerry Landis of University of Dayton Research Institute (UDRI) and Spencer Schweinfurth in assisting sensor manufacture. Final wiring and assembly of the vane and rotor were completed at Florida Turbine Technologies, Inc. (FTT). Digital Impulse Response Algorithms were developed with Dr. Martin Oldfield, University of Oxford. The views and conclusions contained herein are those of the authors and should not be interpreted as necessarily representing the official policies or endorsements, either expressed or implied, of the U.S. Air Force or the U.S. Government.

REFERENCES

[1] Clark, J. P., Polanka, M. D., Meininger, M., and Praisner, T. J., 2006, "Validation of Heat-Flux Predictions on the Outer Air-Seal of a Transonic Turbine Blade", *ASME Journal of Turbomachinery*, Vol. 128, pp. 589-595.

[2] Praisner, T. J., Grover, E. A., Knezevici, D. C., Popovic, I., Sjolander S. A., Clark, J. P., and Sondergaard, R., 2008, "Toward the Expansion of the Low-Pressure-Turbine Airfoil Design Space," ASME Paper No. GT2008-50898.

[3] Clark, J. P., Koch, P. J., Ooten, M. K., Johnson, J. J., Dagg, J., McQuilling, M. W., Huber, F., and Johnson, P. D., 2009, "Design of Turbine Components to Answer Research Questions in Unsteady Aerodynamics and Heat Transfer," AFRL Report No. AFRL-RZ-WP-TR-2009-2180, WPAFB, OH.

[4] Clark, J. P., Koch, P. J., Ooten, M. K., Johnson, J. J., Anthony, R. J., Lemaire, R. P., Kennedy, S. W., White, A. L., Finnegan, J. M., Kobelak, M. D., Johnson, P. D., Huber, F., Downs, J., and Hendershot, J., 2010, "The High Impact Technologies Research Turbine, Build 1," AFRL Report No. AFRL-RZ-WP-TR-2010-2262, WPAFB, OH.

[5] Johnson, J.J., King, P.I., Clark, J.P., Anthony, R. J., Koch, P.J., Ooten, M.K., Kasik, E.A., Ni, R., 2011, "Three-Dimensional Film-Cooled Vane CFD Simulations and Preliminary Comparison to Experiments", *49th AIAA Aerospace Sciences Meeting*, Orlando FL, 4-7 January 2011, AIAA 2011-499.

[6] Epstein, A. and Guenette, G.R. and Norton, R.J.G., 1984, "The MIT Blowdown Turbine Facility," ASME Paper No. 84-GT-116.

[7] Abhari, R.S., Guenette, A.H., Epstein, A.H. and Giles, M.B., 1991, "Comparison of Time Resolved Turbine Rotor Blade Heat Transfer Measurements and Numerical Calculations," ASME Paper No. 91-GT-268.

[8] Shang, T. and Epstein, A. H., 1997, "Analysis of Hot Streak Effects on Turbine Rotor Heat Load," *ASME Journal of Turbomachinery*, Vol. 119, No. 3, pp. 544-553.

[9] Dunn, M.G., 1989. "Phase and Time Resolved Measurements of Heat Transfer and Pressure in a Full-Stage Rotating Turbine", ASME Paper No. 89-GT-135.

[10] Dunn, M.G., Haldeman, C.W., 2004, "Time-averaged Heat Flux for a Recessed Tip, Lip, and Platform of a Transonic Turbine Blade," ASME Paper No. 2000-GT-0197.

[11] Haldeman, C.W., Dunn, M.G., Barter, J.W., Green, B.R., Bergholz, R.F., 2004, "Aerodynamic and Heat-Flux Measurements with Predictions on a Modern one and 1/2 Stage High Pressure Transonic Turbine", ASME Paper GT2004-53478.

[12] Sieverding C.H., Dénos R., Arts T., Brouckaert J.F., Paniagua G., 1998, "Experimental Investigation of the Unsteady Rotor Aerodynamics and Heat Transfer of a Transonic Turbine Stage," VKI Lecture Series on "Blade Row Interference Effects in Axial Turbomachinery Stages".

[13] Didier, F., Denos, R., Arts, T., 2002, "Unsteady Rotor Heat Transfer in a Transonic Turbine Stage," *ASME Journal of Turbomachinery*, Vol. 124, pp. 614, DOI:10.1115/1.1505850

[14] De la Loma, A., Paniagua, G., Verrastro, D., Adami P., 2008, "Transonic turbine stage heat transfer investigation in presence of strong shocks," *ASME Journal of Turbomachinery.* Vol. 130, No. 3, 031019, pp 1-8. July. DOI: 10.115/1.2777193.

[15] Ainsworth, R.W., Schultz, D.L., Davies, M.R.D., Forth, C.J.P., Hilditch, M.A. and Oldfield, M.L.G., 1988, "A Transient Flow Facility for the Study of the Thermofluid-Dynamics of a Full Stage Turbine under Engine Representative Conditions," ASME paper 88-GT-144.

[16] Chana, K., Hurrion, J., Jones, T., 2003, "The Design Development and Testing of a non-Uniform Inlet Temperature Generator for the QinetiQ Transient Turbine Test Facility", ASME 2003-GT-38469.

[17] Marks, C., Sondergaard, R., Wolff, M., Anthony, R.J., 2011, "Experimental Comparison of DBD Plasma Actuators for Low Reynolds Number Separation Control," ASME Paper No. GT2011-45397.

[18] Rabinowicz, J., Jessey, M.E. and Martsch, C.A., 1955. "Resistance Thermometer for Transient High Temperature Studies," *Journal of Applied Physics*, Vol. 23, pp. 97.

[19] Chabai, A.J. and Emrich, R.J., 1955. "Measurements of Wall Temperature and Heat Flow in a Shock Tube," *Journal of Applied Physics*, Vol.26, pp. 779-780.

[20] Vidal, R.J., 1956. *Model Instrumentation Techniques for Heat Transfer and Force Measurements in Hypersonic Shock Tunnels*, Cornell Aeronautical Laboratory Report AD-917-A-1.

[21] Schultz, D.L. and Jones, T.V., 1973. "Heat Transfer Measurements in Short-Duration Hypersonic Facilities," AGARD AG-165.

[22] Jones, T. V., 1995 "The Thin Film Heat Transfer Gauge—A History and New Developments," *Proceedings 4th National UK Heat Transfer Conference*, Manchester, UK, pp. 1–12.

[23] Epstein, A.H., Guenette, G.R., Norton, R.J.G. and Yuzhan, G., 1986. "High Frequency Response Heat Flux Gauges", *Rev. Sci. Instrum*., 57 (4), pp 639-649.

[24] Dunn, M.G., 2001. "Convective Heat Transfer and Aerodynamics in Axial Flow Turbines," ASME 2001-GT-0506.

[25] Haldemann, C. W., Mathison, R. M., Dunn, M. G., Southworth, S. A., Harral, J. W., and Heltland, G., "Aerodynamic and Heat Flux Measurements in a Single-Stage Fully Cooled Turbine--Part II: Experimental Results," ASME Journal of Turbomachinery, Vol. 130, April 2008, pp. 021016-1 to 11.

[26] Illiopoulou, V., Denos., R., Billiard, N., Arts,T., 2004, "Time-Averaged and Time-Resolved Heat Flux Measurements on a Turbine Stator Blade Using Two-layered Thin-Film Gauges," *ASME Journal of Turbomachinery*, Vol.126.

[27] Oldfield, M.L.G., Burd, H.J. and Doe, N.G., 1982. "Design of Wide-Bandwidth Analogue Circuits for Heat Transfer Instrumentation in Transient Tunnels," *Proc. 14th ICHMT Symposium on Heat and Mass Transfer in Rotating Machinery*

[28] Doorly, J.E. and Oldfield, M.L.G., 1987. "The Theory of Advanced Heat Transfer Gauges", *Int. J. Heat Transfer*, vol. 30, No 6, pp. 1159-1168.

[29] Anthony, R.J., Oldfield, M.L.G., Jones, T.V., LaGraff, J.E, 1999. "Development of High Density Arrays of Thin Film Heat Transfer Gauges," *5th ASME/JSME Thermal Engineering Joint Conference*, San Diego, CA. Paper No. AJTE99-6159.

[30] Oldfield, M.L.G., 2006, "Impulse Response Processing of Transient Heat Transfer Gauge Signals", ASME GT2006-90949.

[31] Anthony, R.J, 2006. "Unsteady Boundary Layer Structure on a Leading Edge Subjected to Freestream Turbulence" Presented at 2006 AIAA Fluid Dynamics Conference, San Francisco, CA.

[32] Anthony, R. J., Jones, T. V., LaGraff, J. E., 2005, "High Frequency Surface Heat Flux Imaging of Bypass Transition," J. Turbomach., 127, pp. 241–250.

[33] Anthony, R.J., Jones, T.V., LaGraff, J.E, 2004. "Unsteady surface heat flux under a three-dimensional crossflow boundary layer," AIAA Paper 2004-1344.

[34] Taylor, B.N., Kuyatt, C.E., 1994. "Guidelines for evaluating and expressing the uncertainty of NIST measurement results," NIST Technical Note 1297, 1994 edition.